

4.9, $V_3 = 0.38$, and $V_4 = -0.35$ kcal/mol.

Acknowledgment. This work was supported by the National Science Foundation under Grants CHE78-04258 and CHE81-10541. K. Hagen is grateful to the Norwegian Research Council for Science and the Humanities for partial support and a travel grant.

Registry No. Propenoyl chloride, 814-68-6.

Supplementary Material Available: Tables of total intensities, final backgrounds, average molecular intensities, symmetry coordinates, force constants and wave numbers, and figures equivalent to Figure 2 for 375, 480, and 643 K (44 pages). Ordering information is given on any current masthead page.

Multitechnique Depth Profiling of Small Molecules in Polymeric Matrices

S. J. Valenty,* J. J. Chera, D. R. Olson, K. K. Webb, G. A. Smith, and W. Katz*

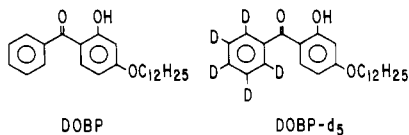
Contribution from Corporate Research and Development Center, General Electric Company, Schenectady, New York 12301. Received January 27, 1984

Abstract: A multitechnique approach has been used to determine the depth profile of a small molecule in a polymeric matrix as a function of heating. The molecule, 2-hydroxy-4-(dodecyloxy)benzophenone, was solubilized in a polyalkylmethacrylate/2-butoxyethanol carrier and applied as a thin film (0.2 μm thick) to the surface of a bisphenol A polycarbonate sheet. Upon heating, the partition of this molecule between the polymethacrylate and the polycarbonate was determined by transmission ultraviolet absorption spectroscopy after selective chemical etching. Infrared attenuated total reflectance sampling showed the disappearance of the substituted benzophenone from a surface layer ca. 0.3–0.4 μm thick. Demonstrated for the first time, the deuterium depth profile obtained by secondary ion mass spectrometry using a deuterated analogue clearly shows the diffusion of this molecule into the polycarbonate interior to a depth of ca. 3 μm . Direct transmission infrared analyses of serially cut microtome slices confirm these observations.

The characterization of a polymer's interfacial region and the study of the chemistry that occurs there are topics of considerable scientific interest and practical importance. For instance, small molecules are added to polymeric matrices to aid processing, prevent photodegradation, reduce flammability, or otherwise enhance the material's overall performance.¹ In a number of cases, the location of such an additive is crucial. As an example, the photodegradation of bisphenol A polycarbonate (PC) is clearly a surface phenomenon² in which any stabilizer added to protect the polymer from light-induced chemistry must be concentrated over or in the PC interfacial region. There are few analytical methods that have been routinely used to map the positions of small molecules in either man-made or biosynthetic polymers such that the resulting molecular distributions might be correlated with the polymer's chemical and physical properties.

We wish to describe a multitechnique approach to determine the in-depth distribution of a topically applied small molecule as a function of subsequent heating. The molecule, 2-hydroxy-4-(dodecyloxy)benzophenone (DOBP),³ a typical UV stabilizer, is initially contained in a thin polyalkylmethacrylate (PAMA) film on the surface of a PC sheet.

DOBP-*d*₅ has three spectroscopically useful labels: a UV chromophore with $\epsilon > 10^4 \text{ M}^{-1} \text{ cm}^{-1}$, an infrared absorbing carbonyl functionality, and deuterium. As analyzed by their



(1) (a) Hawkins, W. L. "Polymer Stabilization"; Wiley-Interscience: New York, 1972. (b) Ranby, B.; Rabek, J. F. "Photodegradation, Photooxidation and Photostabilization of Polymers"; Wiley-Interscience: New York, 1975.

(2) (a) Factor, A.; Chu, M. L. *Polym. Degradation Stab.* **1980**, *2*, 203. (b) Clark, D. T.; Munro, H. S. *Ibid.* **1982**, *4*, 441. (c) Clark, D. T.; Munro, H. S. *Ibid.* **1983**, *5*, 227.

(3) DOBP is a registered trademark of Eastman Chemical Company.

Table I. Selective Chemical Etching: Partition of DOBP as a Function of Heating Time (130 °C)

heating time, min, 130 °C	% DOBP ^a		
	volatilized ^b	in PAMA ^c	in PC ^d
0	0	100	0
2.5	<1	23	76
5	0	17	83
10	11	13	76
15	0	17	83
20	<1	16	83
30	19	10	71
45	8	13	79
60	16	10	74
120	24	7	69
180	33	0	67

^a All absorbances were measured at 292 nm. The initial DOBP absorbance before heating and etching was 0.75. The precision is $\pm 10\%$ of the given value. ^b % DOBP volatilized = ((initial absorbance - absorbance before etching)/initial absorbance)100. ^c % DOBP in PAMA = ((absorbance before etching - absorbance after etching)/initial absorbance)100. ^d % DOBP in PC = (absorbance after etching/initial absorbance)100.

respective methodologies, ultraviolet spectroscopy (UV), Fourier transform infrared spectroscopy (FT-IR), and secondary ion mass spectrometry (SIMS), each of these labels is free of interference from other components of the experimental system. This report correlates the results of these several different techniques which seek an answer to a common question: What is the depth distribution of DOBP? While the example given is quite specific, we feel that in principle the approach is applicable to a wide range of polymeric systems.

Results and Discussion

A. Selective Chemical Etching—UV Analysis. A solution of 2.5 wt % DOBP, 2.0 wt % PAMA, and 95.5 wt % 2-butoxyethanol was flow coated onto a 10-mil PC film and allowed to air-dry for 30 min at room temperature. The differential UV absorption

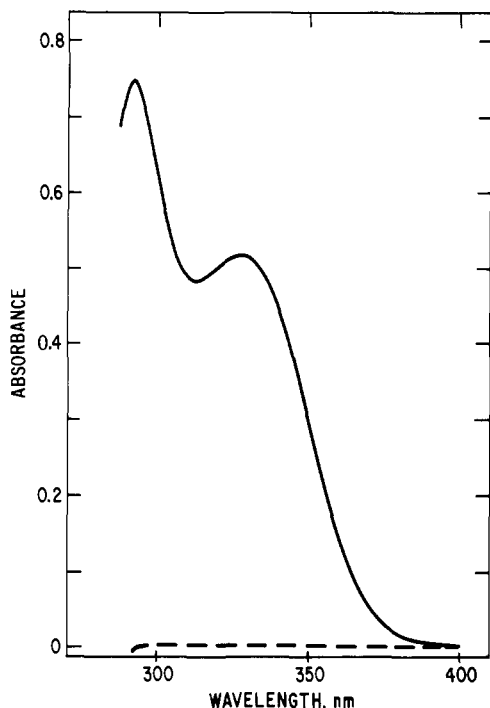


Figure 1. Differential UV absorption spectra of a 10-mil PC film with an air-dried (30 min) DOBP/PAMA coating before (—) and after (---) H_2SO_4 etching.

spectrum of this film vs. an untreated 10-mil polycarbonate film in the reference beam is shown in Figure 1. The absorbance maxima at 292 and 327 nm were used to monitor the amount of DOBP present. In methanol solution, the molar extinction coefficient of the shorter wavelength absorption is $1.51 \times 10^4 \text{ M}^{-1} \text{ cm}^{-1}$.

A simple method in terms of the time and instrumentation required, selective chemical etching, relies on the ability of concentrated H_2SO_4 to depolymerize PAMA while leaving PC untouched under the conditions of the experiment. Treatment of the DOBP-PAMA/PC system prepared above with concentrated H_2SO_4 (2 min, 20–23 °C) completely removes both the DOBP and PAMA as judged by differential UV (Figure 1) and attenuated total reflectance infrared spectroscopy. No physical or chemical change on the PC surface was detected by scanning electron microscopy (SEM) and UV and IR techniques.

After the DOBP-PAMA/PC film was heated in a recirculating air oven at 130 °C for various lengths of time, differential UV spectra were recorded before and after H_2SO_4 etching. The results of a typical experiment are given in Table I. Since the DOBP is thermally stable at this temperature, a decrease in absorbance after heating but before etching suggests its disappearance by volatilization. Any DOBP absorbance remaining after etching indicates the DOBP has diffused into the PC.

While not soluble in water, DOBP does have some solubility in concentrated H_2SO_4 , at least up to ca. $5 \times 10^{-5} \text{ mol/l}$. Upon contact with this acid, 2-hydroxy-4-alkoxybenzophenones turn bright yellow; for instance, the long-wavelength band of DOBP undergoes a 50-nm red shift to 374 nm and ca. $2.5\times$ intensity increase when methanol is replaced by concentrated H_2SO_4 as a solvent. Once the DOBP has permeated into the PC, little (<2%), if any, of it can be extracted during the acid soak and subsequent water rinses. There is no indication of either wavelength shifts or intensity increases for the long-wavelength absorption of DOBP in the UV spectra of films which had been heated for a short time (2.5 and 5.0 min) and acid etched.

These observations suggest that the bulk of the DOBP rapidly diffuses to a depth within the PC that is not accessible to the sulfuric acid. The decrease in total DOBP absorbance at longer heating times prior to etching indicates that back diffusion of DOBP from the PC through the PAMA layer with subsequent volatilization also occurs.

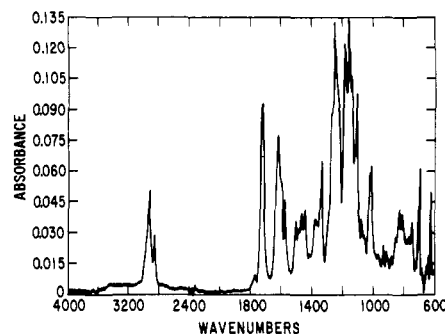


Figure 2. ATR/IR spectrum of an air-dried (30 min) DOBP/PAMA coating on 10-mil PC film prior to heating.

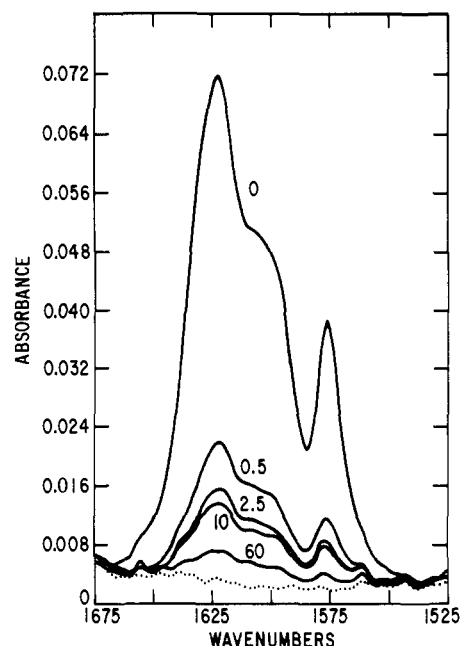


Figure 3. ATR/IR spectra of DOBP-PAMA/PC after heating at 130 °C for 0, 0.5, 2.5, 10, and 60 min and PAMA/PC (...) after heating for 20 min. All spectra shown following subtraction of PC such that the absorption at 1770 cm^{-1} is set to zero.

Table II. Comparison of DOBP Surface Depletion By ATR/IR and UV After Etching

time, min	% DOBP	
	ATR/IR ^a	UV/Etch ^b
0	100	100
2.5	17	23
10	14	13
60	6	10

^aData from Figure 4 (typically $\pm 15\%$ of the given value). ^bData from Table I; % DOBP in PAMA ($\pm 10\%$ of the given value).

B. Infrared Analysis—Attenuated Total Reflectance Sampling. The attenuated total reflectance (ATR) IR spectrum of DOBP-PAMA/PC prior to heating is shown in Figure 2. This spectrum was obtained by using a germanium crystal cut as a parallelepiped shape with a 60° angle. For an index of refraction, $n_D = 1.5\text{--}1.6$, the depth of penetration⁴ in this experiment is ca. $0.3 \mu\text{m}$ within the carbonyl stretch region ($1600\text{--}1800 \text{ cm}^{-1}$) where DOBP (1625 cm^{-1}), PAMA (1735 cm^{-1}), and PC (1770 cm^{-1}) all have strong absorptions.

Within several minutes at 130 °C, almost all of the DOBP absorbance was lost. The contribution of the aromatic ring stretch due to PC at ca. 1600 cm^{-1} has been subtracted from each of the spectra shown in Figure 3 by setting the PC carbonyl stretch

(4) Harrick, N. J. "Internal Reflectance Spectroscopy"; Interscience: New York, 1967.

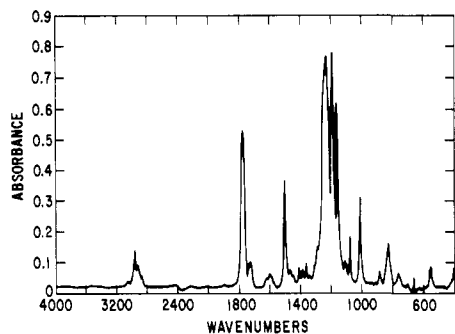


Figure 4. Transmission IR spectrum of KBr-encapsulated first microtome slice (ca. 1.3 μm thick) of DOBP-PAMA/PC after air-drying 30 min but before heating at 130 $^{\circ}\text{C}$.

absorption to zero. The close correspondence between this IR data and the previously obtained UV results is given in Table II. Since the indices of refraction for the various components (2-*n*-butoxyethanol (1.42), PAMA (1.49), PC (1.58), and benzophenone (1.61, model for DOBP)) lie within a narrow range, there will be no significant change ($<\pm 0.02 \mu\text{m}$) in the optical sampling depth as the top-layer composition changes upon heating. Hence, the observed increase in the PC band (1770 cm^{-1}) absorbance can be interpreted as a thinning of the overlying PAMA-DOBP layer. Transmission electron micrographs of transverse sections including the surface region support this observation by showing a 50% decrease in PAMA layer thickness to 0.1 μm as a result of heating the sample at 130 $^{\circ}\text{C}$ for 20 min.

C. Infrared Analyses—Transmission Spectra of Serially Cut Microtome Slices. In contrast to ATR sampling,^{4,5} obtaining the IR spectra of serially cut microtome slices has not been a widely used technique. Priebe, Simak, and Stange⁶ (using 10 μm thick slices) as well as Furneaux and Ledbury⁷ (using 150 μm thick slices) have employed this method to obtain the in-depth concentration of organic functional groups of polymer samples exposed to natural and artificial weathering conditions. In an elegant experiment, Klein and Briscoe studied the diffusion of long-chain carbonyl- and deuterium-containing molecules through bulk poly(ethylene) by moving a microtomed slice (150- μm thickness) across the slit (90- μm width) of a prism IR spectrometer.⁸ In the present work, we find the dimensions of the slice to be analyzed are dependent upon the polymer, the concentration range of the small molecule to be analyzed, the extinction coefficient and the freedom from matrix interference of the absorption band being measured, and the number of scans to be coadded in the FT-IR experiment (practical analysis time). Microtoming PC into 3 mm \times 2 mm \times 2 μm slices, using a 1.5-mm-diameter analysis beam and coadding 1000 scans at 2- cm^{-1} resolution, enables a detection sensitivity for DOBP of ca. 1×10^{-8} mol/ cm^2 . This amount corresponds to ca. 3% of the DOBP originally in the PAMA layer before heating.

A typical transmission IR spectrum of a first or top microtome slice (ca. 1.3 μm thick) for the DOBP-PAMA/PC system before heating is shown in Figure 4. As would be expected, the spectrum is that of PC with additional absorptions due to PAMA and DOBP. We find the use of KBr ($n_D = 1.52$) as an encapsulant to index match the thin polymer slice (PC, $n_C = 1.58$; PAMA, $n_D = 1.49$) invaluable to remove the interference fringes which often preclude the detection of low levels of small molecules in the polymeric matrix. Encapsulation is also useful to flatten and to improve handling of the thin slices.

The IR spectra of the top three serially cut microtome slices from a sample of DOBP-PAMA/PC which had been heated to

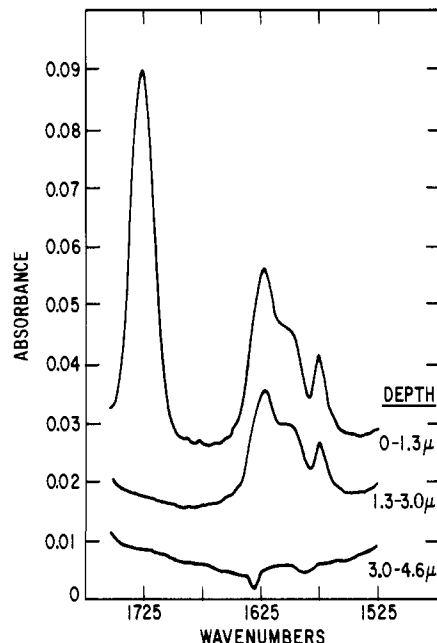


Figure 5. Transmission IR spectra of the first three serially cut microtome slices from a DOBP-PAMA/PC sample which had been heated 10 min at 130 $^{\circ}\text{C}$. All spectra shown following subtraction of PC such that the absorption at 1770 cm^{-1} is ca. zero.

Table III. Distribution of DOBP and PAMA in Taper Cut Microtome Slice of Surface Layer

absorbance (ratio)	analysis location ^a		
	end 1	middle	end 2
PC ^b	0.54 (3.4) ^c	0.26 (1.6)	0.16 (1.0)
PAMA ^d	0.063 (1.0)	0.072 (1.1)	0.065 (1.0)
DOBP ^e	0.029 n(3.2)	0.015 (1.7)	0.009 (1.0)
slice thickness, μm ^f	1.4	0.67	0.41

^a Slice area dimensions: 2 mm \times 3 mm; IR beam diameter: 0.5 mm. ^b 1770 cm^{-1} . ^c Relative absorbance ratios of end 1:middle:end 2, where the absorbance of end 2 was set to 1.0. ^d 1735 cm^{-1} . ^e 1625 cm^{-1} . ^f Slice thickness determined from PC absorbance, 0.39 OD/ μm .

135 $^{\circ}\text{C}$ for 10 min are shown in Figure 5. As indicated, a "bulk" PC slice (obtained ca. 25 μm below the surface) spectrum has already been subtracted from each of these spectra to remove PC absorptions. The top slice (0-1.3 μm) contains all of the PAMA (1730 cm^{-1}) and ca. 60% of the DOBP (1625 cm^{-1}). The remainder of the DOBP is found in the second slice (1.3-3.0 μm) with none observed below 3.0 μm .

IR spectra of thinner top layers can be obtained if the slice is cut as a wedge with an ca. 4:1 taper. Masking the IR beam to a 0.5-mm-diameter spot allows observations of three different thicknesses along the wedge as determined by the calibrated PC carbonyl stretch absorbance, 0.39 OD/ μm . Table III gives the results for one such taper slice cut from a sample heated at 135 $^{\circ}\text{C}$ for 10 min in which the minimum thickness (ca. 0.4 μm) is nearly equivalent to the thickness observed in ATR sampling. Since the DOBP absorbance varies in the same manner as that of PC while the PAMA absorbance remains constant ($\pm 5\%$), it appears that DOBP is uniformly distributed throughout the thickness of the wedge-shaped slice while PAMA is constrained to a layer thinner than the minimum thickness of the wedge (0.41 μm).

The IR results taken on serially cut microtome slices from two DOBP-PAMA/PC samples heated for varying lengths of time at 130 $^{\circ}\text{C}$ are summarized in Table IV. Since the detection sensitivity for DOBP is ca. 3% of its initial absorbance (0.072 OD), less than 3%, if any, of the DOBP has diffused to a depth greater than 3.0-3.5 μm after extended heating. There is fairly close agreement between these IR data and the UV data presented earlier for the total amount of DOBP remaining at any given time.

(5) (a) Allara, D. L. "Industrial Applications of Surface Analysis"; Casper, L. A., Powell, C. J., Eds.; American Chemical Society: Washington, DC, 1982. (b) Willis, H. A.; Zichy, V. J. I. "Polymer Surfaces"; Clark, D. T., Feast, W. J., Eds.; Wiley: New York, 1978.

(6) Priebe, Von E.; Simak, P.; Stange, K. *Kunststoffe* 1972, 62, 105.

(7) Furneaux, G. C.; Ledbury, K. J.; Davis, A. *Polym. Degradation Stab.* 1980-81, 3, 431.

(8) Klein, J.; Briscoe, B. J. *Proc. R. Soc. London, Ser. A* 1979, 365, 53.

Table IV. Distribution of DOBP and PAMA in IR Spectra of Microtomed Slices

time, min ^a	depth, μM^b	IR absorbance			% DOBP remaining		
		PC ^c	PAMA ^d	DOBP ^e	IR ^f	UV ^g	
			Set A				
0	0-2.2	0.85	0.079	0.088	100	100	
0	0-3.5	1.35	0.079	0.082			
2	0-3.0	1.17	0.090	0.079			
	3.0-5.1	0.80	<0.003	0.012	93	>99 ^h	
5	0-2.0	0.79	0.088	0.078			
	2.0-4.6	1.01	<0.003	0.006	88	100	
30	0-2.6	1.03	0.083	0.058			
	2.6-6.4	1.53	<0.003	0.009	75	81	
			Set B				
0	0-2.2	0.85	0.090	0.072	100	100	
	2.2-10	3	<0.004	<0.004			
10	0-1.3	0.51	0.068	0.032			
	1.3-3.0	0.66	<0.002	0.020			
	3.0-4.6	0.63	<0.002	<0.001			
10	0-4.7	1.8	0.068	0.047	84 \pm 9	89	
	4.7-7.8	1.2	<0.002	<0.002			
10	0-5.6	2.2	0.076	0.043			
	5.6-7.1	0.59	<0.005	<0.005			
110	0-3.1	1.2	0.069	0.029			
	3.1-6.4	1.3	<0.002	<0.002			
	6.4-8.8	0.94	<0.002	<0.002	58 \pm 5	76 ⁱ	
110	0-3.5	1.4	0.056	0.028			
	3.5-5.9	0.94	<0.002	<0.002			
	5.9-8.0	0.80	<0.002	<0.002			

^aOven temperature: 130 °C (set A), 135 °C (set B). ^bSlice thickness determined from PC absorbance, 0.39 OD/ μm . ^c1770 cm^{-1} . ^d1735 cm^{-1} . ^e1625-1630 cm^{-1} . ^fAll absorbances of DOBP corrected for variations in PAMA thicknesses by normalizing to average value of PAMA absorbance in each set; A, 0.083 OD; B, 0.071 OD. No variation of PAMA carbonyl stretch before and after drying sample is assumed. ^g% DOBP (UV) = % DOBP in PC + % DOBP in PAMA (from Table I). ^hValue after 2.5 min of heating. ⁱValue after 120 min of heating.

The somewhat lower amounts derived from IR appear to be due to the observed change in the IR spectrum as DOBP crystallizes. While the three carbonyl stretch bands characteristic of DOBP are always observed, there is a shift of maxima for two of the bands from 1615 and 1622 cm^{-1} in solution or PC to 1597 and 1630 cm^{-1} when DOBP in crystalline, respectively. The smallest band at 1576 cm^{-1} is unchanged. In the process, the apparent absorbance of the higher frequency band used for quantitation drops as the separation between the individual bands increases. DOBP crystallization occurs during this same time period as BC evaporates leaving a binary system which phase separates. No phase separation is seen when the sample is heated promptly after the 30-min air-dry period. While the UV and IR/ATR methods can analyze the samples rapidly, the longer preparation time entailed by the microtoming appears to have allowed some crystallization to take place in the $t = 0$ min sample as evidenced by the DOBP carbonyl stretch band structure.

D. Deuterium Depth Profiling by Secondary Ion Mass Spectrometry (SIMS). As an analytical technique, SIMS is unsurpassed in its ability to detect a wide range of elements (hydrogen to uranium) at high sensitivity (ppb-ppm atomic) and provide three-dimensional mapping of elemental composition.⁹ The interaction of a 5-20-keV ion beam with a surface removes, or sputters, species characteristic of that material, e.g., neutral and charged atoms and molecular fragments as well as electrons and photons. SIMS involves a mass spectrometric analysis of these positive and negative atomic and molecular fragments. By monitoring one or more of these secondary ions as material is removed, an in-depth analysis of the sample may be obtained. The key to the profiling capability of SIMS is its shallow sampling depth, ca. 5-50 Å.

While SIMS has found widespread application in inorganic solid-state and semiconductor research,¹⁰ a relatively small number

of papers have involved analyses of organic and biological materials.¹¹ In most of these cases, "static" SIMS (low-primary beam current density and energy) has been employed to detect molecular fragments from only the outermost monolayer(s) in order to obtain "finger print" mass spectra useful for characterizing the organic substrate. The lateral imaging capabilities of static SIMS have been recently demonstrated on organic surfaces by Briggs.¹² Fewer cases have been reported for "dynamic" SIMS (higher primary beam energies and current densities) in which depth profiling of organic polymeric matrices is desired. DiBenedetto and Scola used SIMS to depth profile an incompletely cured silane coating on glass. The SIMS spectra at different depths of penetration revealed that three interphase domains exist, each differing in the concentration of nitrogen and hydrogen present, within a depth of 250 Å from the glass/silane interface.¹³

We report for the first time SIMS in-depth profiling of a deuterated small molecule in an organic matrix over distances of several micrometers. The advantages of using deuterium labeling are twofold: (1) Deuterium at nominal m/e 2 is essentially free of any matrix interferences from the organic materials being studied; in fact, the limit of detection is governed by the natural isotopic abundance of deuterium found in the polymer. The relatively low secondary ion yield for H_2^- and the use of a mass-analyzed primary ion beam to reduce beam contaminants further aid in providing a high S/N ratio for deuterium detection. (2) As for many other labeling applications incorporating deuterium, little perturbation of the chemical system is expected by substituting deuterium for hydrogen. Hence, the rate of diffusion of a relatively large molecule with low deuterium content through a polymeric matrix will be the same as the hydrogen analogue.

A solution of 2.5 wt % DOBP- d_5 and 2.0 wt % PAMA in 94.5 wt % 2-butoxyethanol was prepared, flow coated onto poly-

(9) (a) Evans, C. A., Jr. *Anal. Chem.* **1975**, *47*, 818A, 855A. (b) Katz, W. "Proceedings Microbeam Analysis Society"; Geiss, R., Ed.; San Francisco Press: San Francisco, 1981.

(10) (a) Ryan, M. A.; McGuire, G. E. "Problems and Prospects of Instrumental Surface Analysis of Electronic Materials and Processes"; American Chemical Society: Washington, DC, 1982. (b) Benninghoven, A. "Secondary Ion Mass Spectrometry: SIM III"; Springer-Verlag: New York, 1982.

(11) (a) Benninghoven, A. *Surf. Sci.* **1975**, *53*, 596. (b) Briggs, D.; Wooton, A. B. *Surf. Interface Anal.* **1982**, *4*, 109, 151. (c) Laxhuber, L.; Möhwald, H. *Int. J. Mass Spectrom. Ion Phys.* **1983**, *51*, 93 and references cited therein. (d) Burns, M. S. "Proceedings of the Microbeam Analysis Society"; San Francisco Press: San Francisco, 1982.

(12) Briggs, D. *Surf. Interface Anal.* **1983**, *5*, 113.

(13) (a) DiBenedetto, A. T.; Scola, D. A. *J. Colloid Interface Sci.* **1978**, *64*, 480. (b) Magee, C. W.; Botnick, E. M. *J. Vac. Sci. Technol.* **1981**, *19*, 47.

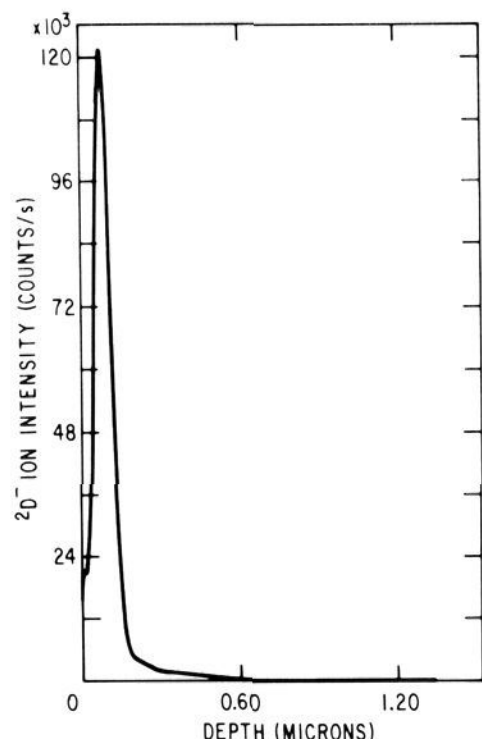


Figure 6. SIMS deuterium ($^2\text{D}^-$) depth profile of Au-coated DOBP- d_5 -PAMA/PC after 30-min air-dry.

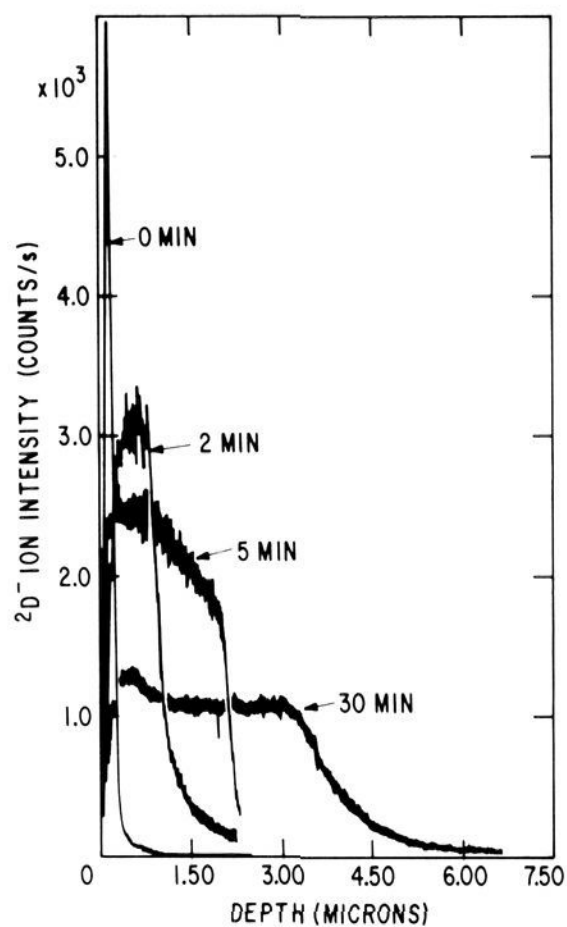


Figure 7. SIMS deuterium ($^2\text{D}^-$) depth profiles of Au-coated DOBP- d_5 -PAMA/PC as a function of heating time (0, 2, 5, 30 min) at 130 °C. As shown, the intensity of the $t = 0$ min profile has been attenuated by a factor of 1/24.

carbonate sheet, and dried at room temperature for 30 min. Assuming a coating density of 1.2 g/cm³, a layer thickness of 0.2 μm , a SIMS sampling area of 60- μm diameter, and 1.3 wt % deuterium content in the DOBP- d_5 , the equivalent weight of deuterium in the area to be analyzed by SIMS is ca. 5×10^{-11} g. After a thin gold coating (ca. 300 Å) was applied by evaporation to minimize charging of the polymer surface, the deuterium profile was measured and is shown in Figure 6. The depth was correlated to the ion sputtering time by measuring the total crater depth with profilometry and assuming a constant sputtering rate (ca. 2.5 Å/s). Note that both the rise and fall of the profile are equally steep with most of the deuterium intensity contained within the half-height width of ca. 0.16 μm . Typically, the thickness of the DOBP-PAMA coating before heating is ca. 0.2 μm as visualized by transmission electron microscopy. Interestingly, the falloff of the deuterium intensity, which presumably marks the PAMA/PC interface, is the same as that obtained for an inorganic

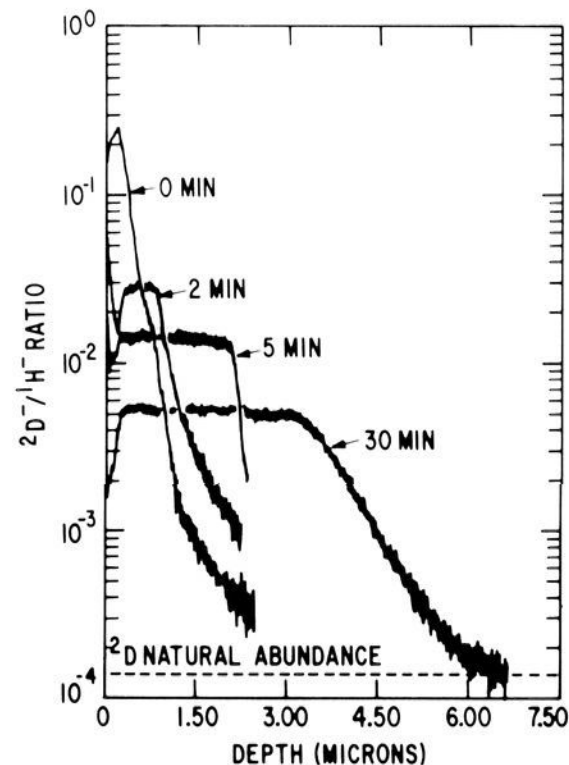


Figure 8. SIMS depth profiles, shown as the log ratio: deuterium ($^2\text{D}^-$) to hydrogen ($^1\text{H}^-$) intensities, of Au-coated DOBP- d_5 -PAMA/PC as a function of heating time (0, 2, 5, 30 min) at 130 °C. The natural abundance of deuterium is 0.015%.

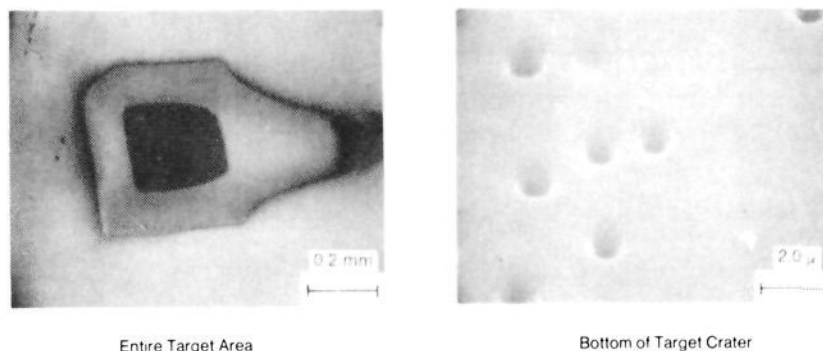


Figure 9. Scanning electron photomicrographs of SIMS crater after ion sputtering ca. 3 μm into the PC.

Pt₂Si/Si interface: 0.02- μm falloff width at 50% loss of intensity and 0.05- μm width at 90% loss. This observation extends the recent report by Laxhuber and Möhwald in which they showed that the chemical composition of an organic model system having three-dimensional order could be determined with a depth resolution of better than 25 Å over relatively shallow depths, ca. 100–150 Å.^{11c}

The deuterium profiles following sample heating at 130 °C for 2, 5, and 30 min are compared to the profile before heating in Figure 7. Note that the intensity of the initial profile is attenuated by a factor of 24 compared to the other three profiles. Hence, there is a rapid DOBP depletion of the surface layer as the deuterated molecules diffuse into the polycarbonate. The extent of this depletion and penetration with time corresponds closely to the results of the IR studies; no significant diffusion below 3.0–3.5 μm is observed.

Another instructive way to display the SIMS data is to plot the ratio of deuterium ion intensity to the hydrogen ion intensity measured simultaneously. The natural abundance of deuterium is 0.015% which corresponds to D/H = 1.5×10^{-4} shown in Figure 8. Note that this log display emphasizes the detection of low levels of deuterium. While the in-depth D/H ratios qualitatively demonstrate a relationship between the diffusion of the deuterated molecule and heating time as shown in Figure 8, there is no quantitative correlation of the integrated deuterium intensity-depth traces with the total DOBP content as judged by UV transmission spectroscopy. The reason for this discrepancy is not currently understood.

Even though ca. 1 to ca. 7 μm of material has been removed to achieve the depth profiles reported here, the sides of the SIMS crater remain sharp as evidenced by both scanning electron microscopy and profilometry, Figures 9 and 10, respectively. The bottom of the crater shows "pitting" and has a surface roughness

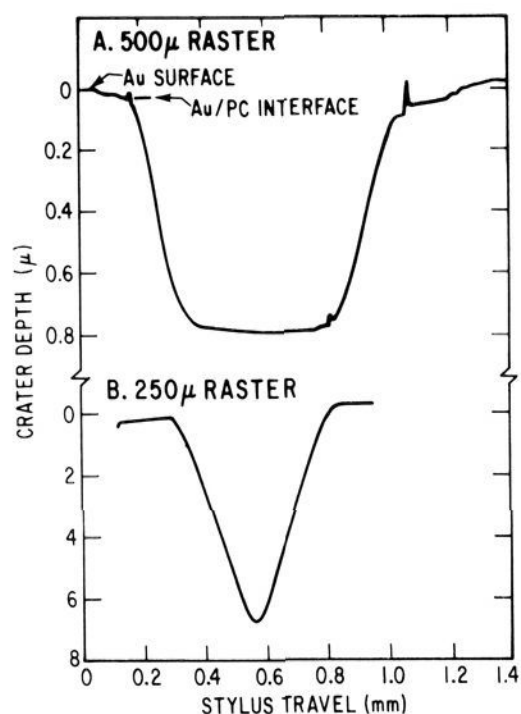


Figure 10. Profilometry traces across the narrow width of typical SIMS craters: (A) 500- μm primary beam raster. (B) 250- μm raster (crater for 30 min profile in Figures 7 and 8).

Table V. Small Spot^a ESCA Analysis of SIMS Crater Floor

sample	atom % C(1s) ^b				atom % O(1s) ^b		C(1s)/O(1s)
	284.6 ^c	286.3 ^d	288 ^e	290.6 ^f	532.5 ^g	534.1 ^h	
PC surface	70	7.4	0	7.1	4.8	10	5.7
SIMS crater 1 ⁱ	61	24	trace	0	13	2	5.7
SIMS crater 2 ^j	68	13	6	0	10	3	6.7

^a X-ray beam diameter: 500 μm (crater 1); 150 μm (crater 2). ^b C(1s) and O(1s) core electron binding energies in eV; typical precision of atom percent composition is $\pm 3\%$ of the value given. ^c C—H, C—C. ^d C—O. ^e C=O. ^f OC(=O)O. ^g O=C. ^h O—C. ⁱ SIMS crater 1: 250- μm raster, 3 μm deep (Au-coated PC surface). ^j SIMS crater 2: 500- μm raster, 1.1 μm deep

of ca. $\pm 0.1 \mu\text{m}$ (crater is $\sim 3 \mu\text{m}$ deep). This roughness will contribute to decreased depth resolution of the elemental profiles with increased bombardment time. In other systems, we have monitored the diffusion of deuterated molecules to depths of ca. 15 μm from the original surface. However, some broadening of the diffusion front is noted which is probably due to a combination of both sputtering effects, i.e., beam-induced heating, and diffusion kinetics. The transmission electron micrograph of a transverse section through the crater floor (ca. 3 μm deep) is shown in Figure 11. The surface roughness does not exceed 0.1–0.2 μm for the areas sampled. One must note that while the secondary ions are primarily emitted from the outer one to two monolayers,^{11c} the damage zone is actually significantly deeper as determined by the projected range of the incident ion beam in a particular matrix. Under the beam conditions used here, the depth of ¹⁶O⁻ penetration in PC is estimated to be ca. 350 Å. The TEM shows a band of morphological structure which is different from that of bulk PC, extending ca. 200–1000 Å below the bottom of the crater floor.

The results of analyzing the SIMS crater floor by small spot ESCA are shown in Table V. There was no change in the overall stoichiometry (C(1s)/O(1s)), indicating little, if any, oxygen incorporation into the PC as a result of the ¹⁶O⁻ bombardment. However, significant changes were observed in the chemical composition of the crater floor vis-à-vis an untreated PC surface: (1) complete loss of carbonate functionality (290.6 eV) and (2) a noticeable increase in C=O concentration (C(1s), 288 eV; O(1s), 532.5 eV). It is interesting to note the comparison between these data and the ESCA analyses of PC surface irradiated with UV light ($\lambda > 290 \text{ nm}$) in an oxygen atmosphere.^{2b} While the carbonate linkage was destroyed in both instances, oxygen incorporation was a significant result of the photolysis experiment alone.

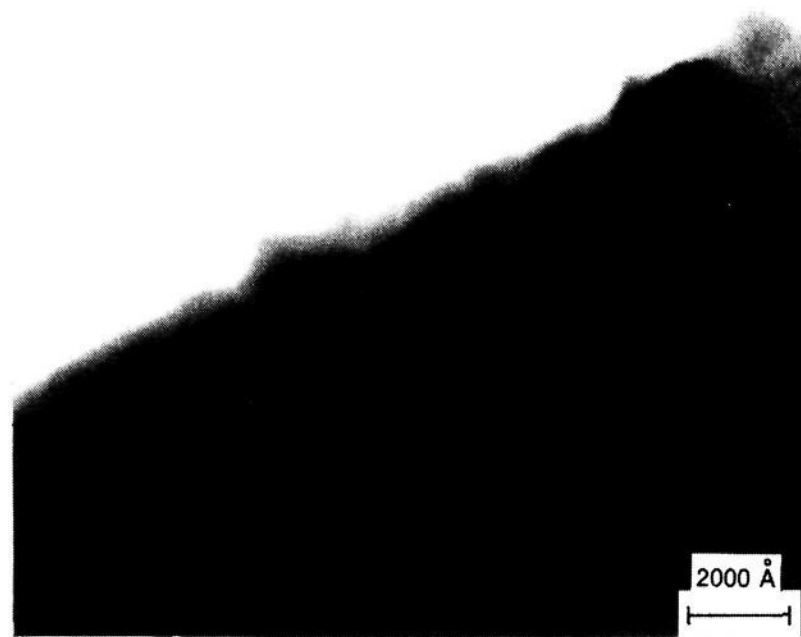


Figure 11. Transmission electron photomicrograph showing a cross-sectional view of the crater floor and the difference in PC morphology immediately below the bottom of the crater.

We speculate that the cross-linking of the matrix and small molecules in advance of the ion-forming region produces the sharp elemental profiles and well-formed craters reported here. If such a situation exists, then one is looking at a material that is not really PC at all but a different substrate in which the positions of the deuterated molecules are stabilized or fixed. In parallel experimentation, it has been shown that bombardment of PC with 2.0-MeV ⁴He⁺ produces a highly cross-linked volume of material extending ca. 5–8 μm below the target area.¹⁴ Cross-linking has also been reported to occur during the UV irradiation of PC.^{2a} Using other polymer systems, Venkatesan and co-workers have demonstrated that ion beam bombardment results in discoloration, loss of molecular species (e.g., hydrogen), and an increase in carbonization of the organic matrix with increasing radiation dose.¹⁵ In selected cases, they propose the use of ion beam irradiation as a means to convert polymer films into inorganic materials.^{15b} An analogous situation is experienced in oxygen bombardment of Si and Ge where the ion-bombarded region forms oxides of the respective matrix. This amorphous oxide layer accounts for the good depth resolution found in these systems. In contrast, other elements (i.e., Co, Ni, Cu), having low-monoxide binding energies (i.e., 2.5–3.5 eV), inhibit the formation of this amorphous region.¹⁶

E. Diffusion of DOBP. Facile diffusion of small molecules through organic polymers is known to occur above the glass transition temperature (T_g).¹⁷ The plasticizing effect of the solvent and DOBP lower the T_g of polycarbonate from its typical value (ca. 149 °C) to one below the oven temperature (130 °C) used in this report; the T_g of PAMA is ca. 68 °C. The extent of diffusion is limited by the rapid volatilization of solvent in the initial minute of heating and the increasingly lower concentration of DOBP as it permeates deeper into the PC. Both of these factors tend to raise the T_g of the PC above its depressed value which

(14) (a) Valenty, S. J.; Chera, J. J.; Smith, G.; Bakhr, H.; Argani, R.; Katz, W. Fifth Biennial Carl S. Marvel Symposium, Tuscon, AZ, March 14–15, 1983. (b) Valenty, S. J.; Chera, J. J.; Smith, G.; Bakhr, H.; Argani, R.; Katz, W. *J. Polym. Sci. Polym. Chem. Ed.*, in press.

(15) (a) Venkatesan, T.; Forrest, S. R.; Kaplan, M. L.; Murray, C. A.; Schmidt, P. H.; Wilkens, B. J. *J. Appl. Phys.* **1983**, *54*, 3150 and references therein. (b) Venkatesan, T.; Wolf, T.; Allara, D.; Wilkens, B. J.; Taylor, G. N. *Appl. Phys. Lett.* **1983**, *43*, 934 and references therein.

(16) Tsunoyama, K.; Suzuki, T.; Konishi, M. "Secondary Ion Mass Spectrometry: SIM III"; Springer-Verlag: New York, 1982.

(17) Johnson, M.; Hauserman, R. G. *J. Appl. Polym. Sci.* **1977**, *21*, 3457.

eventually climbs past the oven temperature, halting any further forward movement of DOBP. The observed migration of DOBP through a low- T_g region back toward the surface and subsequent loss by volatilization will continue at an appreciable rate until the DOBP concentration falls to a level where the T_g once again exceeds the oven temperature.

A satisfactory, simple kinetic treatment of these processes is not possible due to the inhomogeneous and changing chemical composition of the sample surface region. A further complication is attributed to the thermal lag of the PC substrate under the experimental conditions employed. A longer heating time (ca. 0.5–1 min) was required to cause DOBP- d_5 diffusion in the thicker PC sheet (250 mil) usually employed for the SIMS experiments in comparison to the thinner PC films (10 mil) used for the UV/IR (ATR) experiments.

Implications for Other Systems

This paper has illustrated a multitechnique approach to define the in-depth location of a small molecule in a polymer matrix. The use of SIMS to obtain continuous in-depth elemental profiles of deuterated molecules in organic matrices appears to be generally applicable. While the organic substrate obviously suffers "ion beam damage", the crosscorrelation with the UV and IR methodologies reported here suggests that such damage may not preclude the use of SIMS for monitoring the diffusion of deuterated molecules or its imaging capability to visualize structure in synthetic or biological molecular organizes and polymer blends containing only carbon, hydrogen, and oxygen where one domain is enriched in deuterium.

Experimental Section

Materials. 2,4-Dihydroxybenzophenone (DHBP, Uvinul-400, GAF), was recrystallized twice from methanol to give pale yellow needles: mp 145.5–147.0 °C. 2-Hydroxy-4-(*n*-dodecyloxy)benzophenone (DOBP, Eastman Chemicals) was recrystallized sequentially from *n*-hexane and 10% (v/v) ethanol in acetonitrile to give pale yellow needles: mp 50.0–52.0 °C. Polyalkylmethacrylate, PAMA, (DuPont Elvacite 2042 resin) and 2-*n*-butoxyethanol (glycol ether EB, Ashland Chemicals) were used as received. Lexan polycarbonate sheet (250 mm thick) and film (10 mm thick) were obtained from Sheet Products Department (General Electric Co.) and rinsed with isopropyl alcohol prior to use.

Preparation of Deuterated Compounds. For compound identification, infrared spectra (Nicolet 7199C FT-IR), proton magnetic resonance spectra (Varian EM 390, CDCl₃ solution, chemical shifts reported relative to Me₄Si), ultraviolet spectra (Varian Cary 219, $l = 1$ cm), and electron impact mass spectra (Varian-Mat 731) were obtained in a routine manner. Melting points were measured in an open capillary tube contained in an oil bath heated at ≤ 0.5 °C/min and are reported uncorrected.

2',3',4',5',6'-Pentadeuterio-2,4-dihydroxybenzophenone (DHBP- d_5). Benzoic- d_5 acid (4.75 g, 37.3 mmol, Sigma B-8386, 99 atom % D) and resorcinol (4.52 g, 41.0 mmol, Aldrich, 98%) were added to 20 mL of dry nitromethane in a 50-mL flask equipped with a reflux condenser, N₂ purge/static atmosphere inlet, and magnetic stirrer. Boron trifluoride gas (ca. 3.4 g, 50 mmol, Matheson) was slowly bubbled into the flask, causing the suspended solids to dissolve in an exothermic reaction (ca. 35 °C) and give a wine-red clear solution. The solution was stirred at 85 °C for 1 h. The solution volume was concentrated to ca. 10 mL in vacuo. A solution of ca. 10 g of sodium acetate in 25 mL of water was stirred into the viscous red reaction liquid, giving 5.96 g of a yellow solid upon vacuum filtration. The solid was recrystallized from hot methanol/neutral Norit to yield 4.65 g (21.2 mmol, 57% yield) of pale yellow needles: mp 145.5–147.0 °C. Mass spectrum, m/z 219 (molecular ion), 217 (M – 2 H), 137, 110, 82. UV (MeOH): 243 ($\epsilon 1.05 \times 10^4$ M⁻¹ cm⁻¹), 289 (1.37 × 10⁴), 324 (1.02 × 10⁴) nm. IR (CCl₄): 3595, 1631, 1606, 1566, 1511, 1498, 1439, 1388, 1372, 1330, 1316, 1260, 1223, 1190, 1170, 1145, 1101, 979, 917, 843, and 809 cm⁻¹. ¹H NMR (90 MHz, acetone- d_6): δ 6.5 (m, 2 H), 7.5 (d, 10 Hz, 1 H), 12.7 (br s, 1 H).

2',3',4',5',6'-Pentadeuterio-2-hydroxy-4-(*n*-dodecyloxy)benzophenone (DOBP- d_5). Powdered anhydrous K₂CO₃ (1.66 g, 12.0 mmol, Mallinckrodt AR) was added to a solution of DHBP- d_5 (2.14 g, 9.8 mmol) in 50 mL of dry acetone contained in a 100-mL flask equipped with reflux condenser, N₂ gas inlet, and magnetic stirrer. 1-Bromododecane (2.2 g, 2.2 mL, 9.0 mmol, Aldrich B6, 555-1, 98%) was added dropwise to the stirring solution which was then refluxed overnight. After the

solution was cooled in the refrigerator, 2.1 g of a pale pink solid was recovered by vacuum filtration. The yellow semisolid mass remaining after solvent removal was taken up in *n*-hexane, washed with H₂O, dried over Na₂SO₄ and filtered, and the solvent was removed by rotary evaporation leaving a yellow viscous liquid (3.2 g) which crystallized into long needles upon cooling. This solid was purified by silica gel chromatography (hexane/toluene) and recrystallized from MeOH to give 2.2 g (5.7 mmol, 58% yield) of long pale yellow translucent needles: mp 49–52 °C. Mass spectrum, m/z 387 (molecular ion), 219, 217, 137, 110, 82. UV (MeOH): 243 ($\epsilon 9.39 \times 10^3$ M⁻¹ cm⁻¹), 289 (1.39 × 10⁴), 324 (9.39 × 10³) nm. IR (CCl₄): 2928, 2856, 2290, 2275, 1623, 1605, 1574, 1505, 1468, 1389, 1378, 1331, 1248, 1194, 1144, 1101, 918, 810, 805 cm⁻¹. ¹H NMR (90 MHz, acetone- d_6): δ [0.89 (unsym t, $J = 6$ Hz), 1.30 (br s), 1.80 (m, 23 H), 4.10 (t, $J = 6$ Hz, 2 H), 6.45 (m, 2 H), 7.50 (d, $J = 9$ Hz, 1 H), 12.68 (s, 1 H)].

Selective Chemical Etching/Differential UV Spectrometry. Samples of DOBP-PAMA/PC (10-mil film) were dipped into concentrated H₂SO₄ for 1 min at 20–23 °C, removed, rubbed with an acid-wet cotton swab, water rinsed, and dried. This procedure was repeated twice for each sample. A Varian Cary 219 spectrophotometer was used for recording the differential ultraviolet spectra of the treated films vs. an uncoated PC film.

IR Analyses. A Nicolet 7199C FT-IR spectrometer equipped with a liquid N₂ cooled MCT detector was used to record the IR spectra (4000–400 cm⁻¹) of the serially cut and KBr-encapsulated microtome slices. Typically, 1000 scans at 2-cm⁻¹ resolution were obtained for each spectrum. When a Du Pont Sorvall JB-4A microtome with glass knives was used, microtome slices (ca. 3 mm × ca. 3 mm × 2 μ m thick) were cut from a block of DOBP-PAMA/PC (250 mil thick) parallel to the surface. Due to the difficulty of making micrometer-scale adjustments, the first or top slice often was more or less than the nominal 2- μ m thickness. Each slice was weighed on a Mettler M3 microbalance to obtain a measure of slice thickness for the same area dimensions. Slices cut from bulk PC weigh 17–22 μ g. When a PC density of 1.2 g/cm³ and ideal slice dimensions are used, the calculated weight is 22 μ g. After encapsulating in oven-dried KBr powder (1-min evacuation followed by 5 min at 30 000 psi in a 0.5-in.-diameter die) to give a transparent disk, a metal mask with a 1.5-mm-diameter hole was centered on the microtome slice, and this sandwich assembly was positioned in the IR beam. The carbonyl stretch absorbance of PC at 1770 cm⁻¹ was averaged for a number of nominally 2 μ m thick samples weighing 20–22 μ g after cutting 10–15 slices into the polycarbonate and used as a spectroscopic thickness calibration, 0.39 OD/ μ m PC.

ATR spectra of thick and thin polymer samples were obtained by using routine methodology and a germanium crystal (single pass parallel, 60°, 3 mm × 5 mm × 25 mm) in a Harrick Scientific holder.

SIMS Depth Profiling. A Cameca IMS-3f ion microscope was used to obtain the depth profiles. Data were taken by using a mass-analyzed primary beam of ¹⁶O⁻ having an impact energy of 5.5 keV and a current density of ca. 3–5 mA/cm². Secondary ion intensities have been measured by using negative spectrometry to provide maximum sensitivity for the electronegative elements. The pressure in the sample chamber during analysis was 2–3 × 10⁻⁸ torr. In order to obtain optimum depth resolution the primary beam was rastered over an area of $\sim 250 \times \sim 250 \mu$ m with an analyzed area of 60- μ m diameter as limited by the ion beam optics. A 300–500-Å Au overlayer was evaporated on the samples (typically 250 mil thick) to provide a source of slow electrons helping to maintain charge neutrality of the sample surface region during ion bombardment. Sputtering rates (ca. 2.0–2.5 Å/s) were obtained by ratioing the depth of each crater as measured by a Sloan Dektak profilometer to the total profile time.

Miscellaneous. Microscopic analyses were done with a Bausch and Lomb Stereozoom 7 optical microscope, an ISI III scanning electron microscope, or a Hitachi 600 transmission electron microscope after routine sample preparation. The ESCA analysis of the SIMS crater floor was done with a Surface Science Laboratories SSX-100 small spot ESCA at their laboratory in Mountain View, CA.

Acknowledgment. Thanks are due to S. Dorn (GE), E. Koch (GE), and M. Kelly/L. Sharpin/R. Cormia (Surface Science Laboratories) for performing the electron impact MS, TEM, and ESCA analyses, respectively. We thank C. Herderich for the preparation of the typed manuscript. A. Factor and W. V. Ligon, Jr., provided helpful discussion and insight.

Registry No. DOBP, 2985-59-3; PAMA, 9003-42-3; BHBP- d_5 , 91586-06-0; BHBP, 131-56-6; DOBP- d_5 , 91586-07-1; benzoic- d_5 acid, 1079-02-3; resorcinol, 108-46-3; 1-bromododecane, 143-15-7.